Control and navigation system for a fixed-wing unmanned aerial vehicle

Cite as: AIP Advances **4**, 031306 (2014); https://doi.org/10.1063/1.4866169
Submitted: 11 November 2013 • Accepted: 02 January 2014 • Published Online: 12 February 2014

Ruiyong Zhai, Zhaoying Zhou, Wendong Zhang, et al.

Control and navigation system for a fixed-wing unmanned aerial vehicle

Ruiyong Zhai,[1] Zhaoying Zhou,[2] Wendong Zhang,[1,a] Shengbo Sang,[1,b] and Pengwei Li[1]

[1]*MicroNano System Research Centre, Taiyuan University of Technology, Taiyuan 030024, China*

[2]*Department of Precision Instruments and Mechanology, Tsinghua University, Beijing 100084, China*

(Received 11 November 2013; accepted 2 January 2014; published online 12 February 2014)

This paper presents a flight control and navigation system for a fixed-wing unmanned aerial vehicle (UAV) with low-cost micro-electro-mechanical system (MEMS) sensors. The system is designed under the inner loop and outer loop strategy. The trajectory tracking navigation loop is the outer loop of the attitude loop, while the attitude control loop is the outer loop of the stabilization loop. The proportional-integral-derivative (PID) control was adopted for stabilization and attitude control. The three-dimensional (3D) trajectory tracking control of a UAV could be approximately divided into lateral control and longitudinal control. The longitudinal control employs traditional linear PID feedback to achieve the desired altitude of the UAV, while the lateral control uses a non-linear control method to complete the desired trajectory. The non-linear controller can automatically adapt to ground velocity change, which is usually caused by gust disturbance, thus the UAV has good wind resistance characteristics. Flight tests and survey missions were carried out with our self-developed delta fixed-wing UAV and MEMS-based autopilot to confirm the effectiveness and practicality of the proposed navigation method. [http://dx.doi.org/10.1063/1.4866169]

I. INTRODUCTION

In recent years, small fixed-wing unmanned aerial vehicles (UAVs) have been attracting more and more interest, since they are portable, expendable and manoeuvrable. With a short wingspan and light weight, small fixed-wing UAVs can be built easily operated by only one or two persons and can be carried and launched by hand.[1] The UAV market for both military and civilian applications has grown rapidly.[2] Generally, people use UAVs in aerial photography and surveillance, which require steady path-following properties.[3] The navigation system is the major subsystem of a UAV, as it provides the rest of the subsystems with pre-defined position, velocity and attitude information in order to control the aircraft, manage the mission or inform the pilot.[4] In complicated flight terrain, non-linear path-following is also required to perform special tasks and improve flying quality.

A number of trajectory planning and control techniques have been extensively studied for UAVs.[5–14] According to the criterion of minimum energy and minimum manoeuvring, Zhu *et al.* implemented lateral path-following based on the proportional-integral-derivative (PID) feedback method in simulation.[11] Ren considered the problem of constrained non-linear trajectory tracking control to reduce the twelve-state UAV model to a six-state model with altitude, heading, and velocity command inputs.[12] He also proposed designing heading and air speed control commands to

[a]E-mail: wdzhang@tyut.edu.cn
[b]E-mail: sunboa1979@yahoo.com

accomplish the constrained nonlinear tracking control for small fixed-wing UAVs.[13] Luo developed a fractional order $(PI)^{\lambda}$ controller to improve the flight control performance and robustness of a small fixed-wing UAV; the inner closed-loop system of the roll-channel is approximately identified as a first-order plus time delay model using flight test data.[2] Chao *et al.* focused on the design and implementation of a roll-channel fractional order proportional integral (PI^{λ}) flight controller for a small fixed-wing UAV. Time domain system identification methods were used to obtain a simple auto-regressive model of the UAV roll-channel with exogenous input to operate under conditions of wind gusts and payload variations.[14]

This paper describes a low-cost micro-electro-mechanical system (MEMS) based flight control system for small UAVs. The flight control system can be divided into three control loops: damping stabilization control, attitude control and navigation control. The stabilization control, attitude control and longitudinal navigation control loops employ traditional linear PID algorithms to achieve the desired status of the UAV, while the coupling problem of roll damper and heading damper has been considered in stabilization control. In lateral trajectory control, a nonlinear control method was proposed to solve the tracking challenge, which is usually caused by wind. Flight tests and mission results with our self-developed delta wing UAV system show that the proposed navigation method is very effective.

II. FLIGHT CONTROL SYSTEM OF SMALL FIXED-WING UAVs

A. Preliminaries of UAV flight control

The small fixed-wing UAVs' dynamics can be modelled using system states: longitude (p_x), latitude (p_y) and altitude (p_z) for position; u, v and w for velocity; roll (γ), pitch (θ) and yaw (ψ) for attitude; ω_x, ω_y and ω_z for angular rate; a_x, a_y and a_z for acceleration; V_a, V_g for air speed and ground speed; α for the attack angle and β for the slide-slip angle, respectively. The control inputs of small fixed-wing UAVs generally include: aileron (δ_a), elevator (δ_e), rudder (δ_r) and throttle (δ_t). Different types of UAVs may have different control surface combinations. The UAV used in this paper is a small delta fixed-wing aircraft, which adopts flying wing layout with elevators and ailerons without a rudder.

The non-linear equation set below (1)–(3) can be used to model the small fixed-wing UAVs' dynamics.

$$\dot{x} = f(x, u) \tag{1}$$

$$x = [p_x\ p_y\ p_z\ u\ v\ w\ \gamma\ \theta\ \psi\ \omega_x\ \omega_y\ \omega_z]^T \tag{2}$$

$$u = [\delta_a\ \delta_e\ \delta_r\ \delta_t]^T \tag{3}$$

The ultimate objective of flight control is to let the UAV follow a pre-planned 3D trajectory with pre-specified orientations. There are basically two types of controller design approach: the precise-model based nonlinear controller design and the in-flight tuning based PID controller design. The first method requires a precise and complete dynamic model, which is usually very expensive to implement. On the other hand, it is estimated that more than 90% of the current working controllers are PID controllers. Most commercial UAV autopilots use latter cascaded PID controllers for autonomous flight control.

The cascaded PID controller can be used for UAV flight control because non-linear dynamic models can be linear around certain trimming points and be treated as simple single-input and single-output (SISO) or multiple-input and multiple-output (MIMO) linear systems. The UAV dynamics can be decoupled into two modes for low-level control: longitudinal mode and lateral mode. An intuitive controller design to use the classic PID controller structure is as follows:

$$C(s) = K_p(1 + {K_I}/{s} + K_D \cdot s) \tag{4}$$

All the controller parameters (K_P, K_I, K_D) will be determined by either off-line or on-line controller tuning experiments.

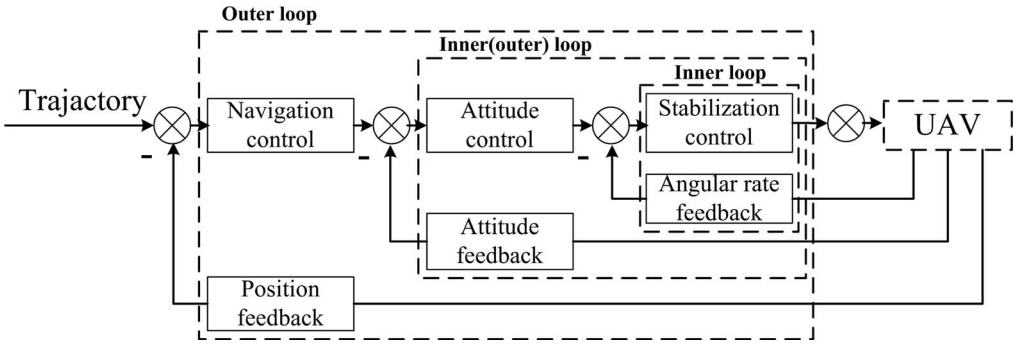

FIG. 1. The basic control principle diagram.

B. Control and navigation law

1. Overall design

In a typical photography or surveillance scenario, the small UAV requires a stable attitude and position control. Therefore, the flight control system, which can be divided into the outer loop and inner loop, as shown in Figure 1, should make the small UAV fly stably.

The inner loop is the stabilization and attitude control loop, which is used as the fundamental control loop to guide the aircraft. The stabilization control is used to increase damping and improve UAV stability. Based on the vehicle's aerodynamics and the sensor information fusion from the accelerometer, gyroscope and Global Positioning System (GPS), the attitude control loop adjusts the elevators and ailerons in real time to correct the roll and pitch angles. The outer loop is a path-following control loop, which acquires heading angle. The navigation loop controls the UAV to eliminate the navigation cross error and heading deviation to complete the tracking task.

2. Stabilization control

The wingspan of the UAV is small, its stability is very poor, and longitudinal control and lateral control need damping systems. Increasing damping and automatically maintaining stability is important and necessary for a UAV to provide a stable platform for attitude and navigation control. The damping stabilization loop is the inner ring of the attitude control loop, whose feedback signal is a tri-axial gyroscope output.

a. Pitch damper. Pitch direction represents the angle between the fore and aft axis of the plane and the ground. The pitch damper is used to improve the longitudinal direction damping, its input signal is the desired pitch angular rate and the output signal is a percentage of the elevator. The feedback of the pitch damper is the pitch angular rate. In order to simplify the control algorithm, but also to prevent drift error caused by integration, the proportional- derivative (PD) controller was adopted:

$$\begin{cases} \Delta\delta_e = K_{Py}e_y + K_{Dy}\dot{e}_y(k) \\ e_y = \omega_y - \omega_{Ey} \end{cases} \tag{5}$$

where, ω_{Ey} and ω_y denote the expected and measured pitch direction angular rate, e_y is angular rate difference, $\Delta\delta_e$ is elevator deviator, K_{Py} and K_{Dy} are the PD control coefficients.

b. Roll damper. Roll direction is the rotation orientation about the centreline of the plane. It is used to describe the tilting motion of the plane when one wing rises or falls in relation to the other. A roll damper is used to improve the lateral direction damping movement. The input signal is the desired roll angular rate and the output signal is the percentage of the aileron. The PD controller was

adopted also to prevent roll integration drift error.

$$\begin{cases} \Delta\delta_a = K_{Px}e_x + K_{Dx}\dot{e}_x(k) + K_{Pz}e_z + K_{Dz}\dot{e}_z(k) \\ e_x = \omega_x - \omega_{Ex} \\ e_z = \omega_z - \omega_{Ez} \end{cases} \tag{6}$$

where, ω_{Ex}, ω_x, e and $\Delta\delta_a$ denote the pitch direction expected angular rate, measured angular rate, angular rate difference and aileron deviator, respectively. The heading angular rate difference e_z is introduced because the roll loop and heading loop are coupled. The roll loop control must be designed to compensate the impact of heading angle because of the coupling.

In order to avoid a large damper control to repress attitude control, the amplitude limit control is needed for pitch damper and roll damper.

3. Attitude control

The attitude control is also divided into pitch loop and roll loop. The expectation of the pitch angle and roll angle controller is given by the height and navigation controller, respectively.

a. Pitch angle control. The pitch angle controller input signal, the expected pitching angle, is given by the altitude controller; the output signal is a percentage of the elevator. It is the inner control of the altitude control. As the dynamic attitude measurement with a certain error, the PD controller was employed for the pitch angle:

$$\begin{cases} \Delta\delta_e^{\theta} = K_p^{\theta}e_{\theta}(k) + K_D^{\theta}\dot{e}_{\theta}(k) \\ e_{\theta}(k) = \theta - \theta^d \end{cases} \tag{7}$$

where ${\Delta\delta_e}^{\theta}$ is elevator percentage, θ^d and θ denote the desired and actual pitch angle, e_{θ} denotes pitch angle control deviation, ${K_P}^{\theta}$ and ${K_D}^{\theta}$ represent the corresponding proportional and differential control coefficients.

b. Roll angle control. The input signal of the roll angle controller is the expected roll angle, and the output signal is the aileron percentage. It is the inner loop of the navigation controller. The control algorithm also uses the PD controller.

$$\begin{cases} \Delta\delta_a^{\gamma} = K_P^{\gamma} \cdot e_{\gamma}(k) + K_D^{\gamma} \cdot \dot{e}_{\gamma}(k) \\ e_{\gamma}(k) = \gamma - \gamma^d \end{cases} \tag{8}$$

where, ${\Delta\delta_a}^{\gamma}$, e_{γ}, γ^d and γ denote ailerons percentage, roll control deviation, and the expected and actual roll angle, respectively. ${K_P}^{\gamma}$ and ${K_D}^{\gamma}$ are the relevant coefficients.

4. Navigation control

Guidance, navigation, and control algorithms are the core of a UAV flight control system to successfully complete the assigned mission through autonomous flight. The performance of the autopilot for trajectory tracking is an important evaluation. The final objective of the UAV is autonomously to perform search, rescue and surveillance missions. Thus, trajectory tracking capability is very useful to allow the UAV optimally to explore the search area. The navigation control can be divided into longitudinal control and lateral control, as shown in Figure 2.

a. Longitudinal control. The longitudinal control employs a traditional linear PID algorithm to achieve the desired altitude of the UAV.

$$\Delta\delta_e^h = K_p^{\theta}\Delta\theta + K_D^{\theta}\Delta\dot{\theta} + K_p^h\Delta h + K_D^h\Delta\dot{h} \tag{9}$$

where, ${\Delta\delta_e}^h$ denotes elevator deflection percentage, Δh denote the difference of current flight altitude and desired flight altitude. The longitudinal control takes pitch angular, pitch angular rate, altitude difference and altitude difference rate as inputs, and the output is elevator deflection.

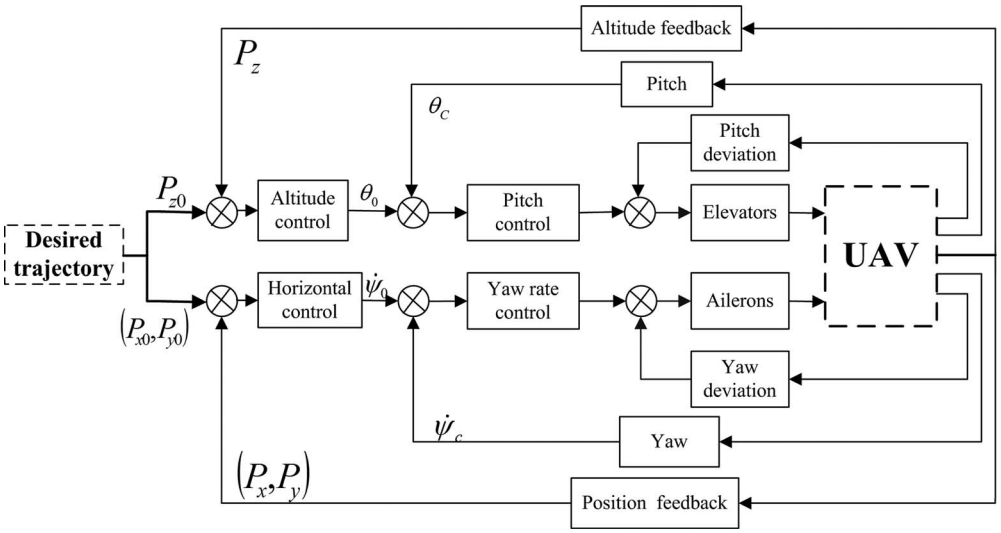

FIG. 2. Navigation control schematic diagram.

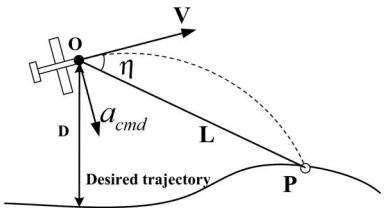

FIG. 3. Nonlinear lateral control for UAVs.

b. Lateral control. Typically, the common method using for lateral control to reduce flight offset is the PD controller. A PD linear controller usually performs well for the outer loop control with careful design, but, with wind influence, it is difficult to achieve satisfactory performance. A lateral non-linear navigation method is presented for horizontal trajectory tracking. When the UAV is in a coordinated turning state, with position, trajectory deflection and ground velocity information obtained from a GPS, the horizontal plane command can be transferred to the expected roll angle to control the lateral loop. As it is flying at low speed, the UAV can automatically adapt to the ground velocity change, the deviation can be corrected and trajectory tracking can easily be realized by this method.

The non-linear guidance control schematic diagram is shown in Figure 3. In order to obtain the lateral control command, the reference point P is selected in the desired trajectory. The requirement is that the length between the reference point and the UAV is a fixed constant. The angle between the velocity vector V and the line L is η., and the lateral control requirement is

$$a_{cmd} = 2V^2 \sin\eta / L \tag{10}$$

By tracking the non-linear overload commands, the UAV can fly along the direction of line L. Due to the velocity change is often caused by wind disturbance, the UAV has good wind resistance flight characteristics. This method is a predictive control method; when the inner loop tracking the guidance instruction, a_{cmd} turns with a circular arc with radius of $R = L/2\sin\eta$, the intersection of the arc and the curve will be point P.

When following a straight line, the navigation deviation D and heading angle deviation η. are smaller and, the above-mentioned non-linear guidance controller is equivalent to a PD. The UAV's tracking results along the desired trajectory are apt to have a certain static error. An integral separation link is introduced to avoid the static error: when path tracking errors are larger, the integration is cancelled to augment system stability; when tracking errors and heading deviations are smaller,

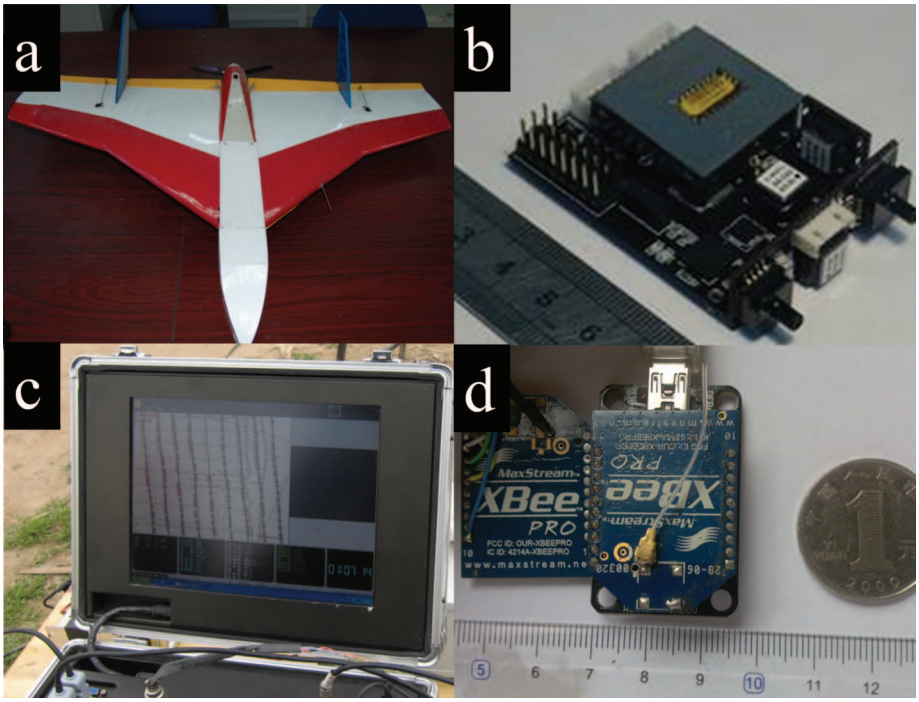

FIG. 4. Components of self-developed UAV platform.

the integral control is used to compensate static errors and improve system control accuracy. The overload command of the horizontal guidance law is revised as follows:

$$a_{cmd} = 2V^2 \sin \eta / L + \alpha \cdot K_I^D \cdot D/s \tag{11}$$

where $K_I{}^D$ is the control parameter in integral part, α is the switch coefficient of the integral term:

$$\alpha = \begin{cases} 1 & |D| < \varepsilon_1; \eta < \varepsilon_2 \\ 0 & |D| > \varepsilon_1; \eta > \varepsilon_2 \end{cases} \tag{12}$$

where, ε_1 and ε_2 are the threshold values of navigation deviation D and heading angle deviation η, which are related to the UAV's flight speed and can be chosen empirically. Then, the inner loop can be controlled via the roll angle, and the control commands can be realized by ailerons and elevators to achieve coordinated turning and to follow the desired path.

III. FLIGHT TEST RESULTS

A. System configuration

The whole navigation system is mainly composed of the UAV, the autopilot, the ground control station (GCS) and the wireless module, which are the flight carrier, the command centre, the observation station and the communication link, as shown in Figure 4.

UAV: The aircraft used here is a self-developed delta fixed-wing UAV TMAV-580. Compared with flapping-wing and rotary-wing UAVs, the fixed-wing UAV is more suitable for search, surveillance and reconnaissance tasks. Its delta wing span is 580 mm and its total weight is 1 kg. It has elevators and ailerons but does not have rudder configuration. The brushless motor is used to provide its motive power. Its cruising velocity is about 25 m/s and endurance time is about 1 hour.

Autopilot: The autopilot is the core of the autonomous system, which guides the UAV to complete desired missions. The self-developed autopilot is an integration of MEMS sensors. It includes an Advanced RISC Machines (ARM) based microprocessor, 3-axis MEMS gyroscopes, 3-axis MEMS accelerometers, 3-axis MEMS magnetometers, a static pressure sensor (altitude), a

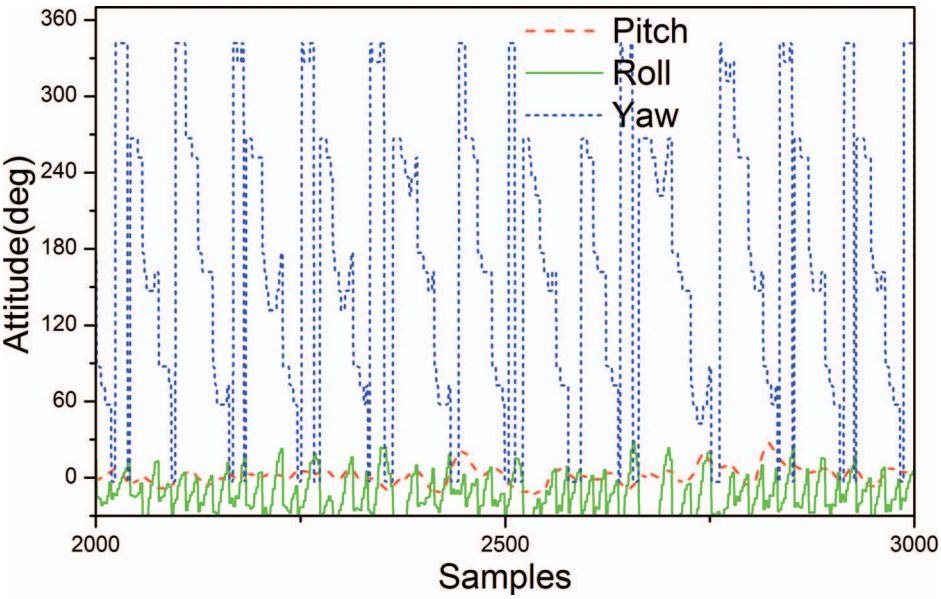

FIG. 5. Altitude information in four-point trajectory.

dynamic pressure sensor (airspeed) and a GPS receiver module. Flight information can be obtained accurately from it, including attitude, height and position. GPS time delay is about 0.4 s, the output frequency of navigation information estimation is 4 Hz.

GCS: The main role of the GCS is to display real-time flight information downloaded from the UAV and to upload various operating commands, such as the operation mode, guidance commands and controller gains. All information of the UAV among the flight experiment tests are displayed in the GCS. The flight control parameters can be set and modified in real flight missions. Ground debugging can be completed and the flight process can be monitored in the GCS.

Wireless module: The wireless module is used for sending and receiving commands between the GCS and the autopilot. In the navigation system, an XBee-PRO 900 module was adopted for data transfer. With radio frequency line-of-sight distances of up to six miles with a high-gain antenna, these modules are ideal for applications requiring low latency and increased data throughput where devices are distributed over great distances.

B. Flight tests

This paper designed a control and navigation system for fixed-wing UAVs. A flight test was implemented to validate its effectiveness. In test, the UAV was trained to follow four pre-arranged points, its velocity was about 25 m/s, the output frequency of the navigation information estimate module was 4 Hz. The navigation system controlled the attitude and made the UAV follow the desired path; the actual pitch, roll and yaw angles information in flight is shown in Figure 5. The four-point trajectory was tracked several times to test the repeatability. The attitude angles of the in-flight mission were regular and periodic. The 3D displacements in tracking the desired trajectory are shown in Figure 6. It could be seen that the lateral deviation of the trajectory was below 20 m and the longitudinal altitude deviation was below 10 m, which satisfied the pre-defined tracking demand.

C. Mission results

The UAV was designated to execute a low-altitude aerial surveillance mission. The mission was to survey a desired 1.5 km $\times$ 0.3 km area in Gong'an county in Jingzhou city in Hubei province, with a camera module as the mission payload. The UAV was launched by a catapult from the red

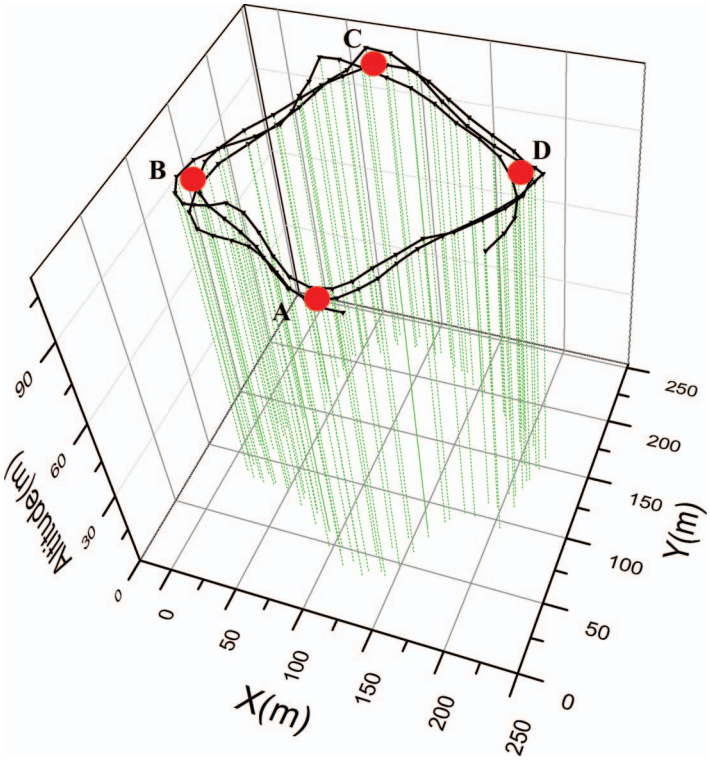

FIG. 6. 3D trajectory results between four points.

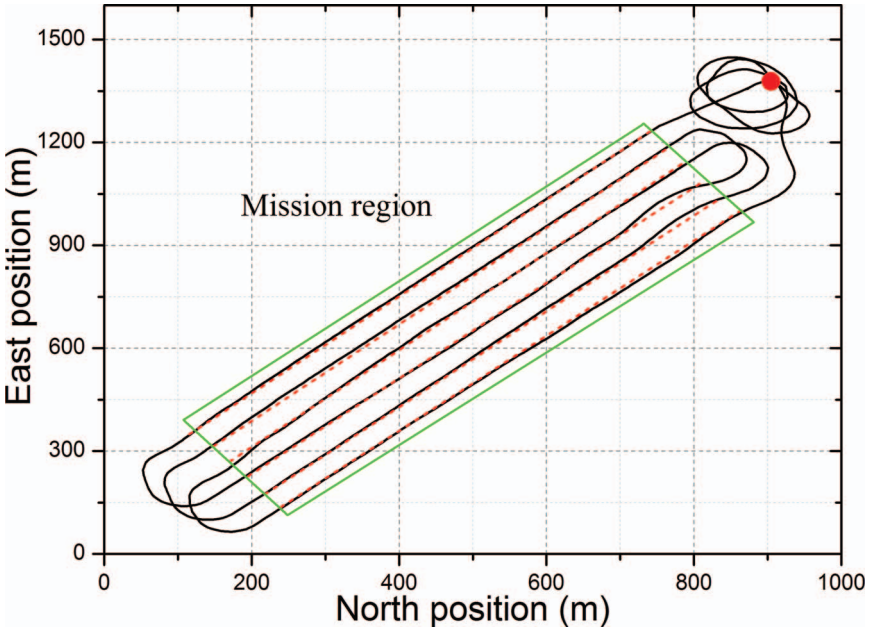

FIG. 7. Lateral plane trajectory information during the missions.

circle region, flying with a spiral climb to the desired altitude, then the pre-arranged flight trajectory was tracked, and the UAV flew back to the starting point. The horizontal navigation information is shown in Figure 7, and the altitude data in Figure 8. The mission was operated under grade 3 wind disturbance; the solid green rhomboid area was the mission region, composed of six trajectory routes. The six short dashed red lines were the desired path, while the black solid lines were the

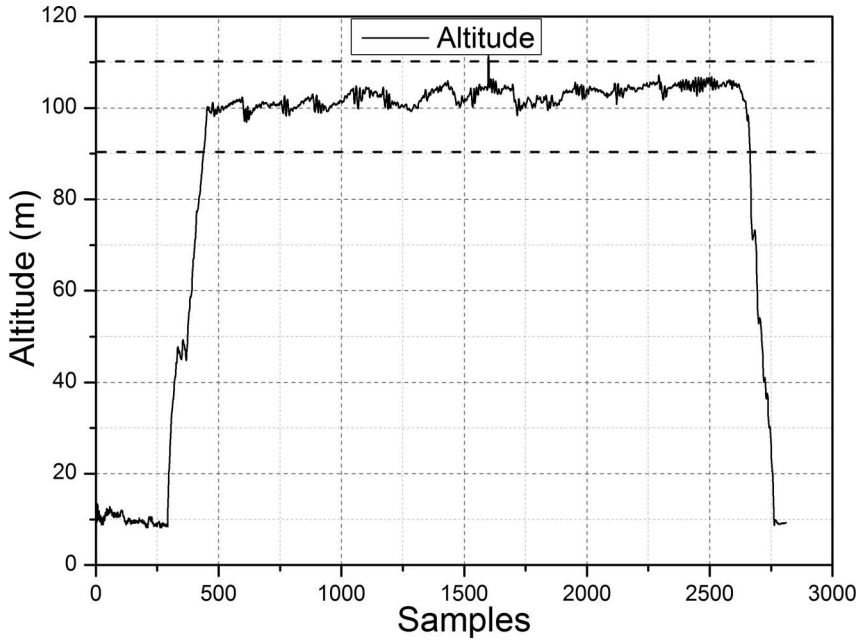

FIG. 8. Altitude information during the missions.

real course. As shown in Figure 7, the path-following information was smooth and continuous, which indicated that the UAV was steady during the flight and the navigation system had better wind resistance dynamic properties. From the lateral position, we can see that the survey trajectory was mostly linear, the trajectory tracking had hardly any overshoot, and the tracking errors were less than 20 m. The altitude was kept at 100 m during the mission, with deviations below 10 m to satisfy the survey requirement. The damping features and steady state errors both met mission requirements.

IV. SUMMARY

The paper presented a flight control and navigation system for small fixed-wing UAVs. In stabilization control, the roll damper control was compensated by heading damper control because of the coupling. The damper control, attitude control and longitudinal navigation control employed traditional linear PID feedback to achieve the desired status of the UAV, and the lateral control used a non-linear control method to complete the planned trajectory. The flight trajectory tracking of the four-point mission was implemented to verify the described navigation control system, and a surveillance mission in Hubei province was undertaken. The flight results indicated that the horizontal and vertical deviations were below the error range and the developed system could guide the UAV to accomplish the desired navigation and surveillance mission.

ACKNOWLEDGMENTS

This work was financially supported by the Science and Technology Major Project of the ShanXi Science and Technology Department (20121101004), Key Disciplines Construction in Colleges and University of ShanXi ([2012]145).

[1] H. Y. Chao, Y. C. Cao, and Y. Q. Chen, Int. J. Control Autom. Syst. **8**, 36 (2007).
[2] Y. Luo, H. Chao, and L. Di, IET Control Theory Appl. **5**, 2156 (2011).
[3] M. A. Goodrich, B. S. Morse, D. Gerhardt, J. L. Cooper, M. Quigley, and C. Humphrey, J. Field Robot. **25**, 89 (2008).
[4] S. L. Parra, and J. Angel, Aerosp. Sci. Technol. **9**, 504 (2005).
[5] G. G. Rigatos, Robot. Auton. Syst. **60**, 978 (2012).
[6] S. Lee, A. Cho, and C. Kee, Aircr. Eng. Aerosp. Tec. **82**, 296 (2010).

[7] Y. Kang and J. K. Hedrick, IEEE T. Contr. Syst. T. **17**, 1202 (2009).
[8] J. C. Fang, C. X. Miao, and Y. H. Du, Industrial Robot. **39**, 475 (2012).
[9] J. Z. Sasiadek, and I. Duleba, J. Intell. Robot. Syst. **29**, 191 (2000).
[10] M. Kumon, M. Nagata, R. Kohzawa, I. Mizumoto, and Z. Iwai, J. Field Robot. **23**, 223 (2006).
[11] R. Zhu, D. Sun, and Z. Y. Zhou, Mechatronics **17**, 245 (2007).
[12] W. Ren and R. W. Beard, IEEE T. Contr. Syst. T. **12**, 706 (2004).
[13] W. Ren, J Intell Robot Syst. **48**, 525 (2007).
[14] H. Y. Chao, Y. Luo, and L. Di, Control Eng Pract. **18**, 761 (2010).